JAAS

PAPER

Cite this: *J. Anal. At. Spectrom.*, 2015, **30**, 1927

A demountable nanoflow nebulizer for sheathless interfacing nano-high performance liquid chromatography with inductively coupled plasma mass spectrometry

Lihuan Shen,[a] Jiannan Sun,[b] Heyong Cheng,*[b] Jinhua Liu,[bc] Zigang Xu[a] and Jinxia Mu[d]

Received 28th May 2015
Accepted 14th July 2015

DOI: 10.1039/c5ja00198f

www.rsc.org/jaas

For direct analyses of micro-samples and the hyphenation with nanoflow separation techniques, a low-cost demountable nanoflow nebulizer was fabricated for inductively coupled plasma mass spectrometry (ICP-MS). A small-bore capillary (20 μm) with a tapered tip served as the sample capillary of the nebulizer. The gas orifice diameter, the internal diameter and the wall thickness at the tip of the sample capillary were 160, 20, and 5 μm, respectively, which ensured stable generation of aerosol by the nebulizer at nanoflow rates down to 50 nL min^{-1} and an ultra-low aspiration rate (80 nL min^{-1}). Narrower aerosol size distribution and higher analyte transport efficiency (nearly 100%) were obtained with the proposed nebulizer than with the previous demountable capillary microflow nebulizer. The sensitivity and detection limit of the proposed nebulizer at 500 nL min^{-1} were about one third of those obtained by using the demountable capillary microflow nebulizer at 5 μL min^{-1}, whereas the precision of the former at 500 nL min^{-1} was even to some extent superior over that obtained with the latter at 5 μL min^{-1}. Furthermore, the ICP-MS instrument could tolerate direct introduction of 100% organic solvents by using the developed nebulizer operating at nanoflow rates. It was utilized to sheathless interface nano-high performance liquid chromatography with ICP-MS for arsenic speciation analysis with good accuracy and precision, proving its strong robustness and good suitability.

1. Introduction

Analyses of micro-volume or nano-volume samples such as clinical, biological and forensic samples have become a growing field of trace element determination by inductively coupled plasma mass spectrometry (ICP-MS).[1] Further interest also includes the analyses of toxic and radioactive samples where the waste should be limited.[1] In these cases, miniaturized sample introduction for ICP-MS is one of the most common approaches. Microflow nebulizers play an important role in the analyses of most micro-samples by ICP-MS but may be ineffective in the analyses of nano-samples, where a nanoflow nebulizer may be a favorable choice for nano-sample introduction into ICP-MS.

Sustainable development gains extensive interest from various fields, which focuses on the activities of human beings and concerns the economy, society and environment. Green analytical chemistry, as the realization of sustainable development in the field of analytical chemistry, is aimed at developing economical, highly efficient and environmentally friendly analytical methodologies.[2,3] Apart from sample preparation, much attention should also be paid to instrumentation, comprising of separation and detection units in greening. As for green liquid chromatography, miniaturization of the column internal diameter below 250 μm is a good strategy to dramatically reduce the sample and mobile phase consumption,[4] which is termed as nano-high performance liquid chromatography (nanoHPLC). Capillary electrophoresis (CE) is another green separation technique since sample consumption and electrolyte flow rate were both at a nanoscale. Highly sensitive and element-specific detectors are usually combined with nanoHPLC or CE for elemental speciation analyses of low-volume samples, among which ICP-MS is one of the best choices. In spite of the powerful capabilities of ICP-MS, its hyphenation with nanoHPLC is often problematic due to flow rate incompatibilities by using conventional nebulizers.

Nowadays, low flow-rate nebulizers are commonly used to replace the conventional nebulizer in sheathing interfacing ICP-MS with nanoHPLC or CE. Diverse pneumatic microflow

[a]*Institute of Analytical and Applied Chemistry, Department of Chemistry, Zhejiang University, Hangzhou, 310027, China*

[b]*College of Material Chemistry and Chemical Engineering, Hangzhou Normal University, Hangzhou, 310036, China. E-mail: hycheng@hznu.edu.cn; Fax: +86-571-28866903; Tel: +86-571-28866903*

[c]*Qianjiang College, Hangzhou Normal University, Hangzhou, 310036, China*

[d]*Department of Environmental Engineering, China Jiliang University, Hangzhou, 310018, China*

nebulizers including high efficiency nebulizers, microconcentric nebulizers, micromist nebulizers, high-efficiency cross-flow micronebulizers, direct injection nebulizers and direct injection high efficiency nebulizers (DIHEN) have been developed for the determination and speciation analyses of low-volume samples.[1] Besides, modified micronebulizers based on tapered sample capillaries including high performance concentric nebulizers,[5] demountable capillary microflow nebulizers (d-CMN)[6] and a heat assisted argon electrospray interfaces[7] were also developed for plasma spectrometry. Recently, Liu *et al.* fabricated a new interface for CE and ICP-MS by the usage of a commercial sprayer kit in electrospray ionization mass spectrometry at 5 μL min^{-1}.[8] However, the addition of an extra makeup flow was necessary owing to the gulf in the liquid flow rate, which led to undesirable dilution of the analyte and degradation of chromatographic resolution.

To overcome the above problem, sheathless coupling of ICP-MS to nanoHPLC/CE is a good strategy. Although micronebulizers might be operated at sub μL min^{-1} flow rates,[9] it is difficult to generate aerosol stably, limiting their applications in nanoflow analysis. A nanoflow nebulizer which can generate stable aerosol is a perfect alternative to micronebulizers as the interface for ICP-MS and CE/nanoHPLC. Schaumlöffel's group presented a pneumatic nanoflow nebulizer (nDS-200) for sheathless interfacing nanoHPLC with ICP-MS.[10] The nebulizer was capable of feeding a wide liquid flow range of 0.05 to 4 μL min^{-1}. The same group soon fabricated an improved nanonebulizer (nDS-200e) by replacing the previous tapered fused-silica needle with an untreated thin 20 μm i.d. fused-silica capillary to reduce back pressure and increase the lifetime of the nebulizer.[11] To further enhance the nebulising efficiency, drop-on-demand aerosol generators based on thermal ink-jets[12,13] and the piezoelectric effect[14] were developed to generate monodisperse pico-liter droplets at frequencies of 1–6.2 kHz (approximately 0.1 to 6300 nL min^{-1}), and the piezoelectric micro-droplet generators are also commercially made available by Microdrop Technologies GmbH.[15] However, their applications may be limited by the high cost and large dead volume of the former. Hence there is still a need for a low-cost and small-dead-volume nanonebulizer for sheathless coupling of ICP-MS and nanoHPLC/CE, which is however scarce in the literature.

In this study, we fabricated a simple, low-cost and small-dead-volume demountable nanoflow nebulizer (d-NN) for stable introduction of liquids at nanoflow rates into ICP-MS based on the demountable capillary microflow nebulizer in our previous work.[6] The tip of the sample capillary of the nanonebulizer was ground with sandpapers to obtain a thin nozzle (5 μm thick and 20 μm i.d.), allowing the generation of fine and stable aerosol at nanoflow rates. The small internal diameter (20 μm) along the whole capillary ensured a small dead volume (≈31.4 nL). Aerosol size distribution and analyte transport efficiency of the d-NN were determined. The nanoflow nebulizer was estimated in terms of the flow rate range, sensitivity, detection limit, precision and self-aspiration rate, and tolerance of methanol and acetonitrile. The feasibility of the nanoflow nebulizer was demonstrated by sheathless interfacing nanoHPLC with ICP-MS for arsenic speciation.

2. Materials and methods

2.1. Chemicals and reagents

All reagents of analytical or chromatographic grade were used. Ultrapure water with a resistivity of 18.2 MΩ cm was prepared from a Milli-Q Plus water purification system (Millipore, Bedford, MA, USA). Sodium arsenate, sodium monomethylarsenate (MMA) and sodium dimethylarsenate (DMA) were purchased from J&K Scientific Ltd (Beijing, China) to prepare 1000 mg L^{-1} of As^{V}, MMA and DMA (as As) in ultrapure water, respectively. Arsenic atomic absorption standard solution of 1000 mg L^{-1} from Sigma-Aldrich (St. Louis, MO, USA) was used as As^{III} standard solution. A 10 μg L^{-1} multi-element solution (Li, Be, Co, Sr, Cd, Ba, Pb, and U) was prepared by diluting 10 mg L^{-1} commercial stock solution (SPEX CertiPrep Inc., USA) with 1% high-purity nitric acid (Sinopharm Chemical Reagent Co., Ltd, Shanghai, China). Sodium tartrate was obtained from Aladdin Chemistry Co., Ltd, (Shanghai, China) to prepare the mobile phase (10 mM sodium tartrate, pH 6.9) with pH adjustment by 1 M tartaric acid or NaOH. 10 μg L^{-1} yttrium served as the internal standard, which was diluted from 1000 mg L^{-1} yttrium (SPEX CertiPrep Inc., Metuchen, USA) in ultrapure water. A certified reference material (CRM) of arsenic species in lyophilized human urine (GBW 09115) from National Standard Material Center (Beijing, China) was used to validate the accuracy for arsenic speciation analysis. All solutions were filtered through membranes of 0.22 μm pore size before analysis.

2.2. Fabrication of the nanoflow nebulizer

The schematic diagram of the nanoflow nebulizer was similar to that of the d-CMN,[6] which is shown in Fig. 1a. It was composed of a nebulizer body, an adapter and a sample capillary. The nebulizer body and adapter were the same as those of the d-CMN except the gas orifice inner diameter (~0.16 mm) at the nozzle. The sample capillary was a 10 cm fused-silica capillary (20 μm i.d. and 360 μm o.d., Yongnian Optic Fiber Factory, Hebei, China) with the tip tapered (Fig. 1b) according to the established procedure by Zhang *et al.*[16] with slight modification. In brief, a 10 cm capillary was carefully cut using a ceramic cleaving stone (Polymicro Technologies, Phoenix, AZ) to obtain a flat section, and the 5 mm polyimide coating at the outlet terminal of the capillary was removed by using a butane flame. After mounting on a hand-held drill, the outlet terminal was rotated at *ca.* 5000 rpm to produce friction with waterproof sandpaper (800 grid) at an angle of 30°. To take away the heat during grinding, several drops of water were added in the contact region on the sandpaper. The wall at the tip was ground to nearly 5 μm thick after a 10 min grinding process. Then, the tapered tip was polished using 1500-grid sandpaper and aluminium oxide polishing powder (R111 Repowder, 0.8–1.2 μm, Gona Powder Technology Co., Shanghai, China) with the same grinding procedure for about 5 min. Finally, the tapered capillary was washed with ultrapure water for 30 min by using a syringe pump. The fabricated tip is illustrated in Fig. 1c. The wall thickness at the tip end was about 5 μm. The capillary annulus area and gas annulus area were calculated to be

0.000314 and 0.0194 mm^2, respectively. The nanonebulizer was assembled according to our previous work.[6] The tapered capillary was inserted into the hole of the adapter and then they were inserted into the nebulizer body cautiously. Both joints were sealed by small amounts of epoxy resin and the tip of the tapered capillary was adjusted flush with the nozzle tip of the body under a microscope. Then, the whole nebulizer was left alone on a platform for 6 h until epoxy resin was hardened.

2.3. Instrumentation

An argon ICP-MS (X Series^{II}, Thermo Fisher Scientific Inc., USA) was operated in the time-resolved analysis mode for the detection of arsenic at a mass isotope of 75. The conventional sample introduction system of ICP-MS was replaced by the fabricated nanoflow nebulizer coupled with a heated single pass spray chamber (heated to 90 °C).[17,18] Adjustment of pH was performed with the assistance of a HI 98128 pH-meter (Hanna Instrument, Italia). A syringe pump (Model 35-2226, Harvard Apparatus Inc.) equipped with a 10 mL syringe was employed to continuously feed solutions to the nanoflow nebulizer. The operation conditions of ICP-MS were daily optimized by maximizing the intensity of ^{7}Li, ^{59}Co, ^{111}In, ^{208}Pb and ^{238}U using a continuous flow of 10 μg L^{-1} standard solution at 500 nL min^{-1} before the hyphenation, which are listed in Table 1. For comparison, the previous demountable capillary microflow nebulizer[6] was also used in combination with the same heated single pass spray chamber.

NanoHPLC separation of arsenic species was performed using a strong anion exchange capillary column (SAX, 3 μm, 100 μm i.d. × 365 μm o.d. × 25 cm long). The capillary column was packed in the laboratory according to the procedure by Zhang's group.[19,20] A nanoliter sample was injected into the nanoHPLC column using a Model C4-1004 nano-injection valve (Valco Instruments, Houston, TX, USA) with a 50 nL rotator. Sample loading into the internal sample loop was manually achieved using a 1 μL flat-needle syringe. A flow rate of 980 nL min^{-1} for the nanoHPLC separation was supplied by a conventional high-pressure pump (Model PU-985, 0.01–5 mL min^{-1} flow rate range, Jasco, Japan) at a flow rate of 0.1 mL min^{-1} by flow splitting. The splitting tubing was a 60 cm fused silica capillary (50 μm i.d. and 365 μm i.d., Yongnian Ruifeng Optical Fabric Factory, Hebei, China). Two side arms of a PEEK tee (Unimicro (Shanghai) Technologies Co., Ltd., Shanghai, China) were connected to the splitting tubing and the outlet tubing of the high-pressure pump while the remaining side arm was connected to the nano-injector *via* a 5 cm PEEK tubing (64 μm i.d. and 1.59 mm o.d.). The mobile phase waste from the splitting tubing was reused by inserting the splitting tubing into a bottle. The separation of arsenic species was carried out by using 10 mM sodium tartrate at pH 6.9 in an isocratic mode. The connection of the column and the nanoflow nebulizer was achieved *via* a PEEK microfingertight union of 5 nL internal volume for 360 μm o.d. tubing (Part no. P-772) from Upchurch Scientific (Oak Harbor, WA). The separation column was equilibrated with the mobile phase at a flow rate of 620 nL min^{-1} for at least 1 h before separation.

Table 1 Operating conditions of the nanoHPLC-ICP-MS system

Parameters	Value
ICP-MS system	
RF power, W	1200
Sampler cone (orifice diameter, mm)	1.1
Skimmer cone (orifice diameter, mm)	0.9
Cooling gas, L min^{-1}	13.02
Auxiliary gas, L min^{-1}	0.75
Nebulizer gas, L min^{-1}	d-NN: 0.88 d-CMN: 0.95
Nebulizer gas backpressure, bar	d-NN: 2.1 d-CMN: 1.9
Solution uptake rate, μL min^{-1}	d-NN: 0.05–5.0 d-CMN: 5.0
Isotope monitored	^{75}As, ^{89}Y
Dwell time, ms	100
Data acquisition mode	Time resolved analysis
nanoHPLC system	
Capillary column	SAX (3 μm, 100 μm i.d. × 360 μm o.d. × 25 cm long)
Mobile phase	10 mM sodium tartrate, pH 6.9
Flow rate of mobile phase, nL min^{-1}	360 to 1510
Sample loop, nL	50

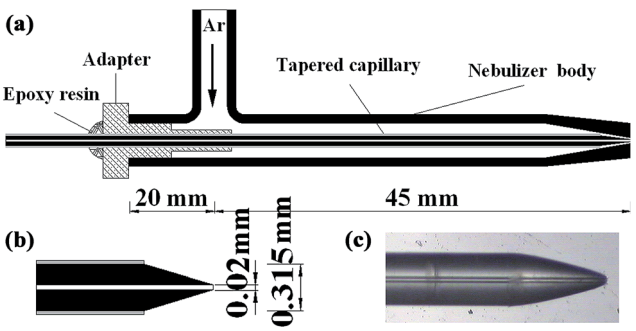

Fig. 1 Schematic diagram of the demountable nanoflow nebulizer (a), enlarged diagram of the nozzle (b) and the photograph of the fabricated tip (c). The dimensions are given in mm.

2.4. Determination of aerosol size distribution and analyte transport efficiency

Droplet size distributions of primary aerosols from the d-NN and the d-CMN were estimated by a simple experiment according to the literature.[21] In brief, a sheet of pH test paper (4 cm × 4 cm, pH 1.4–3.0, Aladdin Chemistry) was placed 20 mm from the nebulizer gas nozzle tip perpendicular to the centerline of the aerosol. A 2% HNO_3 solution was individually sprayed by the two nebulizers to the pH test paper at sample uptake rates of 500 nL min^{-1} and 5 μL min^{-1}, respectively. The sprayed volume was controlled to be 10 μL. All the original

recordings were photographed by using a Huawei Honor 3C mobile and processed by Adobe Fireworks CS4.

Transport efficiencies (the ratio of analyte mass flux delivered to the plasma to the analyte mass uptake rate) for the d-NN were determined according to the direct filter collection method.[21] Cellulose nitrate membrane filters (0.22 μm pore size, 50 mm diameter, Sinopharm Chemical Reagent) were employed to trap the analyte. The aerosol was generated through spraying a 10 mg L^{-1} multi-element solution at sample uptake rates of 500 nL min^{-1} and 5 μL min^{-1}, respectively. The tertiary aerosol at the outlet terminal of the transport tube was entirely carried to the filter by an aspirated air flow at 12 L min^{-1}. The spraying time was constant at 20 min. The filters were then extracted with 10 mL of 1% HNO_3 for 30 min. Pumping of the same volume of the solution directly into the filter was also performed and the filter was also extracted with 10 mL of 1% HNO_3 for 30 min. The extracted solutions were determined using ICP-MS, and the transport efficiencies were calculated as the percent ratios of the net signal intensities for the filter collections to those for the corresponding direct collections.

3. Results and discussions

3.1. Structural features of the nanoflow nebulizer

The objective of this work is to sheathless couple nanoHPLC to ICP-MS using a pneumatic nanoflow nebulizer for better resolution and higher sensitivity than sheathing nanoHPLC-ICP-MS interfaces. The pneumatic nebulization of liquid into aerosol is usually achieved by the Venturi effect due to the argon expansion after a narrow orifice. To generate a fine and stable aerosol at nanoliter flow rates, a liquid flow of high velocity at the exit is necessary to interact with the high-velocity nebulising gas, which can be obtained by dramatically decreasing the internal diameter of the sample capillary at the tip. The small internal diameter of 20 μm at the tip led to a high velocity of the liquid flow (~1.1 cm s^{-1} at 200 nL min^{-1}) in the tip, which was comparable to that obtained by using the Meinhard conventional concentric nebulizer operating at 0.1 mL min^{-1}. Besides, the small wall thickness of the tip resulted in highly efficient gas–liquid interactions, facilitating the formation of small droplets. In combination with a low dead-volume single pass spray chamber (a chamber inner volume of 3.8 mL) heated to 90 °C, the aerosol was immediately evaporated and 100% transported into the plasma without any liquid waste.[18,22,23] Moreover, the sample capillary of the nanoflow nebulizer could be replaced by a new tapered capillary conveniently.[6,24] The hardened epoxy resin became soft after immersing into boiling water and the assembled nebulizer could be disassembled readily. Such an arrangement ensured low cost for fabrication and maintenance.

The difference between d-NN and d-CMN lied on the sample capillary though the structure of the proposed d-NN was similar to that of the d-CMN. A small-bore capillary of entirely 20 μm i.d. with a tapered tip was used for the d-NN while a large-bore capillary of entirely 250 μm i.d. with a tapered tip only at the exit was used for the d-CMN. Therefore, the proposed d-NN offered some advantages over the d-CMN. First, the d-NN could generate stable aerosols at nanoscale flow rates and showed higher sensitivities and lower detection limits than the d-CMN (see the following Sections 3.2 and 3.3). Secondly, the self-aspiration rate of the d-NN was downscaled from 4.77 μL min^{-1} of d-CMN[6] to 80 nL min^{-1} (see the following Section 3.2). Therefore, the laminar flow in capillary electrophoresis induced by the suction effect would be dramatically decreased and the resolution was hence improved. Thirdly, the dead volume of the d-NN was about 31.4 nL, which was decreased by at least 100-fold in comparison with d-CMN (4.91 μL). The low dead volume of the nebulizer decreased the time for eluted analytes retaining in the nebulizer, and thus peak broadening was reduced.

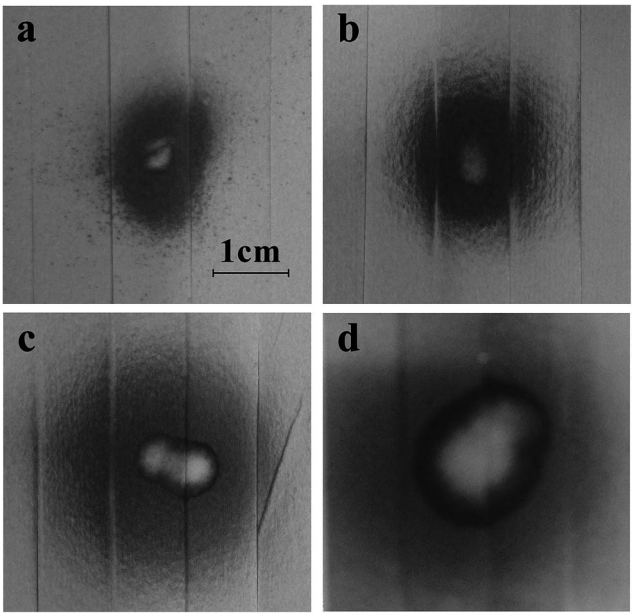

Fig. 2 Comparison of the aerosols generated by the d-NN ((a) 500 nL min^{-1} and (b) 5 μL min^{-1}) and d-CMN ((c) 500 nL min^{-1} and (d) 5 μL min^{-1}).

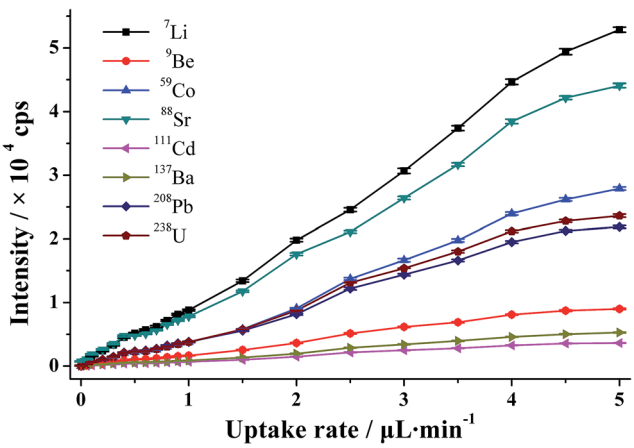

Fig. 3 Signal intensity as a function of sample uptake rate for the nanoflow nebulizer operating at a nebulizer gas flow rate of 0.88 L min^{-1}, and the concentration of the multi-element solution was 10 μg L^{-1} in 1% HNO_3 for each element.

Table 2 Detection limits, sensitivities and precisions for d-NN and d-CMN

		Detection limit (ng L^{-1})		Sensitivity (Mcps/mg L^{-1})		Precision (%RSD)		
		d-NN	d-CMN	d-NN	d-CMN	d-NN		d-CMN
Mass		0.5 μL min^{-1}	5 μL min^{-1}	0.5 μL min^{-1}	5 μL min^{-1}	0.5 μL min^{-1}	5 μL min^{-1}	5 μL min^{-1}
Li	7	15.4	6.2	0.43	1.5	2.7	0.74	4.8
Be	9	20.3	8.4	0.084	0.31	3.0	0.65	4.1
Co	59	6.7	1.7	0.28	0.95	3.2	0.58	3.9
Sr	88	5.8	1.6	0.49	2.1	2.1	0.42	4.2
Cd	111	27.4	10.2	0.034	0.16	2.8	0.62	4.0
Ba	137	15.3	6.4	0.047	0.15	2.6	0.69	3.8
Pb	208	7.2	2.2	0.16	0.59	2.7	0.48	4.4
U	238	6.5	2.1	0.19	0.66	3.1	0.75	5.1

Furthermore, the total analytical time might be accordingly reduced.

3.2. Aerosol size distribution and analyte transport efficiency

Aerosols comprising of small and uniform droplets moving at similar velocities are definitely desirable in ICP spectrometries. The quality of the primary aerosols by the d-NN and the d-CMN at different sample uptake rates was examined and the results are shown in Fig. 2. Three main conclusions could be made. First, the geometric dimensions of the photograph obtained with the d-NN were far smaller than those obtained with the d-CMN at the same uptake rate. Secondly, the black dot distributions in the photographs for the d-NN were uniform and focused compared with those for the d-CMN. Thirdly, droplet size distributions of the aerosol by the d-NN were to some extent narrowed with the sample uptake rate. The above three observations indicated that radial velocities of the droplets from the d-NN were lower and more uniform than those from the d-CMN.

The transport efficiencies of the d-NN measured by the direct filter collection method were 93.2–98.6% at 500 nL min^{-1} and 84.6–91.3% at 5 μL min^{-1}. In comparison, the analyte transport efficiencies of the d-CMN were about 51.8–66.0% at 500 nL min^{-1} and 27.5–42.2% at 5 μL min^{-1}. The transport efficiencies of the d-NN decreased with the sample uptake rate and were significantly superior to the d-CMN, which was in good accordance with the droplet distribution in Fig. 2. An analyte transport efficiency of nearly 100% was achieved with the d-NN. This agreed well with the observation of no deposition of liquid on the internal wall of the spray chamber with the d-NN at sample uptake rates less than 5 μL min^{-1} over a 2 h period. All these results proved the high-quality of the aerosol produced by the d-NN.

3.3. Sample uptake rate, sensitivity, precision and self-aspiration rate

Liquid introduction into the plasma was performed by using the nanoflow nebulizer with a multi-element standard solution containing ^{7}Li, ^{9}Be, ^{59}Co, ^{87}Sr, ^{111}Cd, ^{137}Ba, ^{208}Pb and ^{238}U in 1% HNO_3 at flow rates ranging from 50 to 5000 nL min^{-1}. As shown in Fig. 3, the intensities of the eight elements increased gradually with the liquid flow rate over the tested range. Higher flow rates were restricted by the high back pressure (in excess of the tolerance of the syringe pump). We then estimated the analytical performance of the nanonebulizer with respective to detection limit and sensitivity (Table 2). It was also found that the intensities obtained with the nanonebulizer at 500 nL min^{-1} accounted for 21–31% of those obtained with d-CMN at 5 μL min^{-1}. This indicated that the transport efficiency of the nanonebulizer was improved by about 2–4 times over d-CMN, which was in good accordance with the results in Section 3.2.

The relative standard derivations (RSDs) of the signals were gradually decreased from 6.2–8.3% to 1.6–2.8% with the liquid flow rate from 50 to 1000 nL min^{-1}. The RSDs of the intensities were all superior to 4.0% at flow rates above 0.6 μL min^{-1}. In comparison with our previously developed d-CMN, the proposed d-NN offered better precisions (Table 2). The RSDs obtained by using the d-NN at 500 nL min^{-1} were improved by about 24–49% in comparison with those of the d-CMN at 5 μL min^{-1}. As shown in Table 3, the precisions of the proposed nanflow nebulizer were comparable to those of the nDS-200e nebulizer[11] but dramatically superior to those of the nDS-200 nebulizer,[10] d-DIHEN[9] and inkjet-based drop-on-demand aerosol generator,[12] demonstrating the powerful capacity of the

Table 3 Comparison of signal precisions of nanonebulizers

Nebulizer	Isotope	RSD (%)	Ref.
nDS-200	^{89}Y	21.5% at 50 nL min^{-1} 4.1% at 450 nL min^{-1}	10
nDS-200e	^{166}Er	8.2% at 50 nL min^{-1} 2.3% at 500 nL min^{-1}	11
d-DIHEN	^{7}Li, ^{51}V, ^{55}Mn, ^{59}Co, ^{63}Cu, ^{75}As ^{103}Rh, ^{115}In, ^{133}Cs, ^{232}Th, ^{238}U	3.7–7.1% at 900 nL min^{-1}	9
Inkjet-based aerosol generator	^{115}In	7.9% at 60 nL min^{-1} 4.7% at 590 nL min^{-1}	12
d-NN	^{7}Li, ^{9}Be, ^{59}Co, ^{88}Sr, ^{111}Cd, ^{137}Ba, ^{208}Pb, ^{238}U	6.2–8.3% at 50 nL min^{-1} 2.1–3.2% at 500 nL min^{-1}	This work

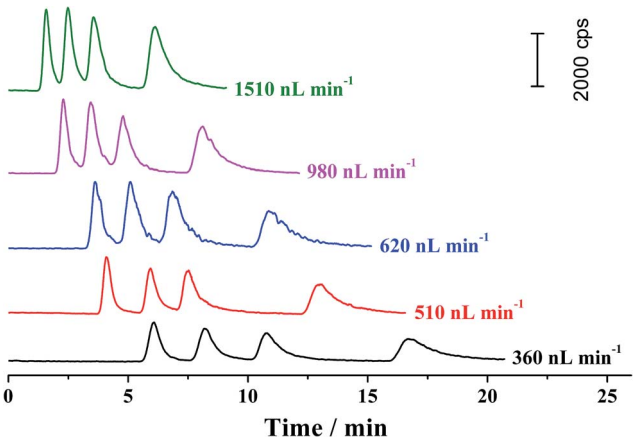

Fig. 4 Chromatographic separations of As^{III}, As^{V}, MMA and DMA in 500 μg L^{-1} by nanoHPLC-ICP-MS at various mobile phase flow rates. Peaks are in the increasing time order of As^{III}, MMA, DMA and As^{V}.

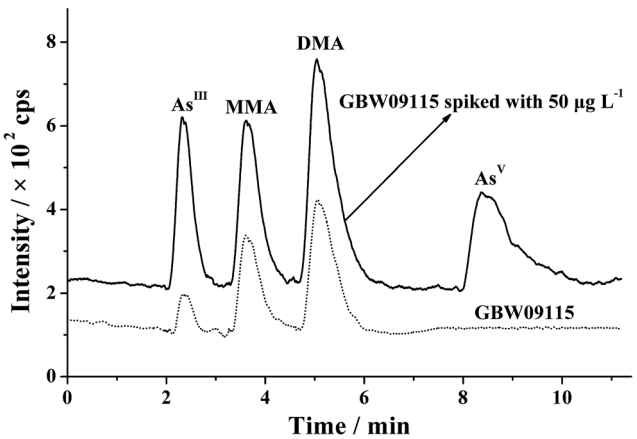

Fig. 5 Typical chromatograms of arsenic species in GBW09115 as well as the spiked solution (spiked with 50 μg L^{-1}). An isocratic elution was performed at a mobile phase flow rate of 980 nL min^{-1}.

nanoflow nebulizer in generating stable aerosol at nanoliter per minute flow rates. Just because of satisfactory precision and high transport efficiency of the d-NN, the detection limits of the d-NN at 500 nL min^{-1} were comparable to those of the d-CMN at 5 μL min^{-1}. The experimental results implied high transport efficiency of the nanoflow nebulizer over a wide flow rate range, indicating its feasibility in the hyphenation of ICP-MS with capillary and nanoHPLC and CE sheathlessly.

The self-aspiration rate of the nanonebulizer was measured according to the method described in the literature.[21] After diminishing the natural evaporation of ultrapure water, its self-aspiration rate was about 80 nL min^{-1}, which was far less than that of d-CMN (4.77 μL min^{-1}). It is worth noting that the free aspiration rate of the nanoflow nebulizer was even lower than the typical electroosmotic flow rate in CE, demonstrating its potential in interfacing CE with ICP-MS.

3.4. Effect of methanol and acetonitrile on the signal intensity

In reversed-phase liquid chromatography, methanol and acetonitrile are the typical eluting reagents. The use of a high-proportion organic solvent usually has a detrimental effect on the ICP stability at normal flow rates (about 0.5–2 mL min^{-1}) but an enhancement effect on the signal at microliter flow rates.[10] Effects of methanol and acetonitrile on the ICP-MS intensities at a flow rate of 500 nL min^{-1} were investigated. From the experimental results it was found that the intensities of the eight elements were slightly enhanced (by about 2–16%) with methanol/acetonitrile ranging from 0% to 100%. Considering the subsequent application of the nanoflow nebulizer, effects of methanol and acetonitrile on the ^{75}As signal at a flow rate of 500 nL min^{-1} were also estimated. There was a gradual increase in the intensity of ^{75}As with the proportion of methanol/acetonitrile ramping up to 60%, where the intensity of ^{75}As was enhanced by about 2.6 fold. This effect could be ascribed to a carbon-based charge-transfer reaction in the plasma.[25] The above results demonstrated the strong tolerance of organic solvents (~100%), indicating that the organic mobile phases could be directly introduced into the plasma without any strategy such as dilution and the addition of oxygen gas in nanoHPLC-ICP-MS for a short term use. However, direct introduction of 100% organic solvents into the plasma for long-term use of the nanonebulizer might still suffer from carbon build-up, and hence it might be recommended to add oxygen gas of a minute amount into the plasma to burn out the redundant carbon. However, the enhancement effect by organic solvents used in nanoHPLC might also result in some problems in accurate quantification. For nanoHPLC operating under isocratic elution, the carbon load of the plasma was constant. By contrast, the carbon load would keep pace with the composition of the organic solvent along the gradient elution process. Considering the effect of the organic solvent on the ^{75}As signal, a gradient related change of the ^{75}As signal might be encountered according to Pröfrock and Prange,[26] and hence accurate

Table 4 Contents of As-species in GBW09115 by the nanoHPLC-ICP-MS method ($n = 3$)

Analyte	Determined value (μg L^{-1})	Spiked (μg L^{-1})	Found (μg L^{-1})	Recovery (%, $n = 3$)	Certified value (μg L^{-1})
As^{III}	10.8 ± 0.4	50	57.2 ± 2.5	93 ± 4	11.4 ± 0.2
MMA	17.1 ± 0.9	50	63.1 ± 2.2	92 ± 3	15.4 ± 1.2
DMA	59.5 ± 2.4	50	105.9 ± 2.3	93 ± 5	64.4 ± 4.5
As^{V}	Not detected	50	47.2 ± 2.0	94 ± 2	Not certified

quantification might be problematic. On the occasion, the application of constant[27–29] and matched reversed gradient[26] post-column sheathing flows to partly compensate or completely mask the change of the composition of the organic solvent during the gradient process was described, although both strategies might be at a high risk of sacrificing sensitivity owing to the dilution effect by the sheathing flow.

3.5. Performance of the nanonebulizer in sheathless coupling of nanoHPLC and ICP-MS

The feasibility of the nanoflow nebulizer in sheathless coupling of nanoHPLC and ICP-MS was demonstrated by arsenic speciation analysis. A comparison experiment on individual separation of four arsenic species (As^{III}, MMA, DMA and As^{V}) by sheathless and sheathing nanoHPLC-ICP-MS using the nanoflow nebulizer was carried out. In comparison with the chromatograms obtained for sheathing nanoHPLC-ICP-MS (a post-column sheathing flow of 5 μL min^{-1}), the peak heights of the As-analytes for sheathless nanoHPLC-ICP-MS were significantly enhanced (by 3.1–5.5 fold), indicating the higher sensitivity of the sheathless interface. Then, the nanoflow nebulizer was utilized as the sheathless interface for nanoHPLC-ICP-MS at various mobile phase flow rates (Fig. 4). As the mobile phase flow rate increased, the signal intensity was enhanced, which agreed well with the results from Fig. 3. This indicated satisfactory suitability of the nanoflow nebulizer for sheathless interfacing nanoHPLC with ICP-MS in a wide flow rate range. The reproducibility of the sheathless interface was demonstrated by three replicate determinations of the arsenic species in terms of chromatograms. The precisions of retention time, peak height and peak area were in the ranges of 0.8–1.7%, 2.3–3.8%, and 2.8–4.4%, respectively. All these results proved the robustness of the developed nanoflow nebulizer for the sheathless interface of nanoHPLC and ICP-MS. Analysis of a urine reference material (GBW 09115) as well as its spike recovery test was performed to validate the accuracy of the nanoHPLC-ICP-MS method (Fig. 5 and Table 4). Considering the constant carbon load of the plasma under isocratic elution in this work, the quantification of the arsenic species was completed by using the peak area using an external calibration method. The determined concentrations of all arsenic species agreed well with the certified values, and good recoveries (92–94%) were also achieved, proving its accuracy.

4. Conclusions

In this work, we fabricated a low-cost demountable nanoflow nebulizer for sheathless coupling of nanoHPLC and ICP-MS. By usage of a tapered small-bore capillary as the sample capillary, the proposed nanoflow nebulizer offered some advantages such as low dead volume, high transport efficiency, ultra-low self-aspiration rate and satisfactory analytical performance. The proposed nanoflow nebulizer allowed stable introduction of microsamples at flow rates in the nanoliter per minute range and enabled a robust sheathless coupling of nanoHPLC and ICP-MS. Application of sheathless nanoHPLC-ICP-MS for arsenic speciation analysis showed the potential of the developed nebulizer in the hyphenation of other nanoflow separation techniques (*i.e.* CE, MCE) and ICP-MS.

Acknowledgements

The authors acknowledge the financial support from the National Natural Science Foundation of China under project Nos 21275038, 21405030 and 21205109, the Analysis and Measurement Foundation of Zhejiang Province under project Nos 2014C37094 and 2014C37100, and the Scientific Research Foundation of Zhejiang Provincial Department of Education under project No. Y201430445.

References

1 J. L. Todolí and J. M. Mermet, *Spectrochim. Acta, Part B*, 2006, **61**, 239–283.
2 L. H. Keith, L. U. Gron and J. L. Young, *Chem. Rev.*, 2007, **107**, 2695–2708.
3 M. Tobiszewski, A. Mechlinska and J. Namiesnik, *Chem. Soc. Rev.*, 2010, **39**, 2869–2878.
4 J. Płotka, M. Tobiszewski, A. M. Sulej, M. Kupska, T. Górecki and J. Namieśnik, *J. Chromatogr., A*, 2013, **1307**, 1–20.
5 K. Inagaki, S.-i. Fujii, A. Takatsu and K. Chiba, *J. Anal. At. Spectrom.*, 2011, **26**, 623–630.
6 H. Cheng, X. Yin, Z. Xu, X. Wang and H. Shen, *Talanta*, 2011, **85**, 794–799.
7 R. G. Brennan, S. A. Rabb, K. Jorabchi, W. F. Rutkowski and G. C. Turk, *Anal. Chem.*, 2009, **81**, 8126–8133.
8 L. Liu, B. He, Z. Yun, J. Sun and G. Jiang, *J. Chromatogr., A*, 2013, **1304**, 227–233.
9 R. G. Brennan, S.-A. E. O'Brien Murdock, M. Farmand, K. Kahen, S. Samii, J. M. Gray and A. Montaser, *J. Anal. At. Spectrom.*, 2007, **22**, 1199–1205.
10 P. Giusti, R. Lobinski, J. Szpunar and D. Schaumlöffel, *Anal. Chem.*, 2006, **78**, 965–971.
11 C. Rappel and D. Schaumloffel, *J. Anal. At. Spectrom.*, 2010, **25**, 1963–1968.
12 J. O. O. v. Niessen, J. N. Schaper, J. H. Petersen and N. H. Bings, *J. Anal. At. Spectrom.*, 2011, **26**, 1781–1789.
13 J. O. O. v. Niessen, J. H. Petersen, J. N. Schaper and N. H. Bings, *J. Anal. At. Spectrom.*, 2012, **27**, 1234–1244.
14 S. Groh, P. K. Diwakar, C. C. Garcia, A. Murtazin, D. W. Hahn and K. Niemax, *Anal. Chem.*, 2010, **82**, 2568–2573.
15 http://www.microdrop.de/.
16 T. Zhang, Q. Fang, W. B. Du and J. L. Fu, *Anal. Chem.*, 2009, **81**, 3693–3698.
17 H. Cheng, Z. Xu, J. Liu, X. Wang and X. Yin, *J. Anal. At. Spectrom.*, 2012, **27**, 346–353.
18 X. Han, H. Y. Cheng and Z. G. Xu, *J. Anal. Sci., Methods Instrum.*, 2012, **31**, 180–184.
19 Q. Liu, L. Yang, Q. Wang and B. Zhang, *J. Chromatogr., A*, 2014, **1349**, 90–95.
20 B. Zhang, Q. Liu, L. Yang and Q. Wang, *J. Chromatogr., A*, 2013, **1272**, 136–140.

21 J. Li, T. Umemura, T. Odake and K.-i. Tsunoda, *Anal. Chem.*, 2001, **73**, 1416–1424.
22 G. Caumette, C. P. Lienemann, I. Merdrignac, H. Paucot, B. Bouyssiere and R. Lobinski, *Talanta*, 2009, **80**, 1039–1043.
23 M. Grotti, F. Ardini and J. L. Todolì, *Anal. Chim. Acta*, 2013, **767**, 14–20.
24 Y. Takasaki, K. Inagaki, A. Sabarudin, S.-I. Fujii, D. Iwahata, A. Takatsu, K. Chiba and T. Umemura, *Talanta*, 2011, **87**, 24–29.
25 G. Grindlay, J. Mora, M. de Loos-Vollebregt and F. Vanhaecke, *Spectrochim. Acta, Part B*, 2013, **86**, 42–49.
26 D. Pröfrock and A. Prange, *J. Chromatogr., A*, 2009, **1216**, 6706–6715.
27 P. Giusti, D. Schaumlöffel, J. R. Encinar and J. Szpunar, *J. Anal. At. Spectrom.*, 2005, **20**, 1101–1107.
28 A. P. Navaza, J. R. Encinar and A. Sanz-Medel, *Angew. Chem., Int. Ed.*, 2007, **46**, 569–571.
29 A. P. Navaza, J. R. Encinar, M. Carrascal, J. Abian and A. Sanz-Medel, *Anal. Chem.*, 2008, **80**, 1777–1787.